Cancer Letters 442 (2019) 161–169

Contents lists available at ScienceDirect

Cancer Letters

journal homepage: www.elsevier.com/locate/canlet

Original Articles

Histone deacetylase inhibitor panobinostat potentiates the anti-cancer effects of mesenchymal stem cell-based sTRAIL gene therapy against malignant glioma

Seung Ah Choi[a,b,c], Chanhee Lee[a,b,c], Pil Ae Kwak[a,b,c], Chul-Kee Park[c], Kyu-Chang Wang[a,c], Ji Hoon Phi[a,b,c], Ji Yeoun Lee[a,c,d], Sangjoon Chong[a,b,c], Seung-Ki Kim[a,b,c,*]

[a] Division of Pediatric Neurosurgery, Pediatric Clinical Neuroscience Center, Seoul National University Children's Hospital, Seoul, Republic of Korea
[b] Adolescent Cancer Center, Seoul National University Cancer Hospital, Seoul, Republic of Korea
[c] Department of Neurosurgery, Seoul National University Hospital, Seoul National University College of Medicine, Seoul, Republic of Korea
[d] Department of Anatomy, Seoul National University Hospital, Seoul, Republic of Korea

ARTICLE INFO

Keywords:
hAT-MSC.sTRAIL
Panobinostat
Malignant glioma
Antitumor effect
Apoptosis

ABSTRACT

Human adipose tissue-derived mesenchymal stem cells expressing the secreted form of the tumor necrosis factor-related apoptosis-inducing ligand (hAT-MSC.sTRAIL) have demonstrated therapeutic activity against various tumors in preclinical studies. However, the limited expression of TRAIL death receptors remains a challenge. We evaluated the therapeutic efficacy of panobinostat in enhancing the sensitivity of hAT-MSC.sTRAIL-mediated apoptosis in malignant glioma. Panobinostat effectively inhibited all malignant glioma cells (IC_{50}, 0.03–0.23 μM), enhancing the expression of DRs, but not in hAT-MSCs. Combined treatment with hAT-MSC.sTRAIL and panobinostat significantly suppressed cell viability and enhanced apoptosis. In a diffuse intrinsic pontine glioma (DIPG) mouse model, the combined treatment induced decreases in tumor volume and prolonged survival. Our study demonstrates that panobinostat enhances the expression of TRAIL DRs and potentiates the anti-cancer effects of hAT-MSC.sTRAIL.

1. Introduction

Malignant glioma is one of the most aggressive cancers and is frequently resistant to conventional anti-cancer treatments [1]. Among malignant gliomas, diffuse intrinsic pontine glioma (DIPG) that arises from the brainstem is especially inoperable and has a dismal prognosis [1–5]. In 2016, the World Health Organization (WHO) classification of tumors of the central nervous system underwent major reconstruction of the classification of brain tumors with an emphasis on molecular profiles. In accordance with new molecular profiles, the majority (~80%) of cases that would have traditionally been diagnosed as DIPG harbor a new genomic diagnosis of 'diffuse midline glioma, H3 K27M-mutant' [6,7]. Lysine to methionine (K27M) mutations in the histone H3.1 and H3.3 genes result in broad epigenetic dysregulation, including globally decreased K27 methylation and increased K27 acetylation [8]. Therefore, an epigenetic modifying agent is currently being studied as a therapeutic candidate for DIPG [7,9].

Tumor necrosis factor-related apoptosis-inducing ligand (TRAIL) selectively induces apoptosis in tumor cells specifically without harming normal cells [10–12]. Previous studies have identified 4 membrane-bound TRAIL receptors: TRAIL death receptor (DR) 4, DR5, decoy receptor (DcR) 1 and DcR2. Binding of TRAIL to the functional domains of DR4 or DR5 activates a signaling pathway that ultimately leads to apoptosis [13]. Decoy receptor (DcR) 1 and DcR2 appear to act as 'decoys' for their ability to inhibit TRAIL-induced apoptosis when overexpressed [13]. Despite its selectivity, apoptosis led by TRAIL DRs was not as powerful as envisioned due to the low expression level of TRAIL DRs in glioma. Combined treatment with histone deacetylase inhibitors (HDACi) has been attempted as a treatment alternative [11,12,14–17].

The action of HDACi such as a suberanilohydroxamic acid (SAHA, vorinostat), valproic acid (VPA) and panobinostat in malignant glioma has been an area of active research [15,18,19]. HDACi induces anti-tumor effects through multiple mechanisms such as the production of reactive oxygen species, activation of apoptotic pathways, and suppression of immune evasion [18,20]. HDACi also has the ability to

* Corresponding author. Division of Pediatric Neurosurgery, Seoul National University Children's Hospital, 101 Daehak-ro, Jongno-gu, Seoul, 03080, Republic of Korea.
E-mail address: nsthomas@snu.ac.kr (S.-K. Kim).

https://doi.org/10.1016/j.canlet.2018.10.012
Received 25 January 2018; Received in revised form 25 September 2018; Accepted 9 October 2018

sensitize TRAIL by inducing DR4 and DR5 [15–17]. These receptors modulate the sensitivity of TRAIL-resistant tumor cells and further enhance the apoptosis-inducing potential in breast carcinoma, bladder tumors, and melanoma [17,19,21]. Among various HDACi, we chose panobinostat in this study because it was the most effective against diffuse midline glioma, H3 K27M-mutant both *in vitro* and *in vivo* [7]. Panobinostat was also approved by the Food and Drug Administration (FDA) for clinical use in multiple myeloma patients in 2015, and multiple clinical trials are also ongoing for other cancers [22]. Furthermore, panobinostat can cross the blood–brain barrier (BBB) [23].

We previously confirmed that human adipose tissue-derived mesenchymal stem cells expressing the secreted form of the tumor necrosis factor-related apoptosis-inducing ligand (hAT-MSC.sTRAIL) show therapeutic efficacy in a xenograft brainstem glioma mouse model [14]. Herein, we evaluate the expression of DRs after panobinostat treatment and demonstrate the therapeutic potential of the combined treatment of hAT-MSC.sTRAIL with panobinostat on malignant glioma.

2. Materials and methods

2.1. Cell cultures

Fresh glioblastoma tumor tissues and adipose tissues were collected from patients after obtaining written informed consent from themselves or their parents; this protocol was reviewed and approved by the Institutional Review Board (IRB) of the Seoul National University Hospital (IRB #1501-054-640). Primary cultured glioblastoma cells (World Health Organization Grade IV) were obtained from two patients (SNUH.GBM1: a 64-year-old man, glioblastoma, IDH-mutant; SNUH.GBM2: a 55-year-old woman, glioblastoma, IDH-wild-type) who underwent surgical excision. These patients did not receive neoadjuvant therapies. The cells were isolated as reported previously [24] and used under 4 passages in this study. The cells were cultured in Dulbecco's modified Eagle's medium (DMEM; WelGENE, Daegu, Korea) supplemented with 10% fetal bovine serum (FBS; Gibco, Grand Island, NY) and 1% antibiotic/antimycotic. Diffuse midline glioma, H3 K27M-mutant primary cells (DIPG XIII: H3.3 K27M and DIPG XIX: H3.3 K27M) were obtained from Dr. Michelle Monje (Stanford University) and cultured according to an established protocol [25]. Human glioblastoma cell lines (U87 and U251: no IDH1 mutation) were purchased from the American Tissue Culture Collection (ATCC, Manassas, VA).

Human adipose tissues were collected from the anterior chest subcutaneous fat during operations for vagus nerve stimulation for intractable epilepsy. Cells isolated from adipose tissues were cultured as previously described [14]. All cells were incubated at 37 °C in a humidified atmosphere of 5% CO_2.

2.2. Characterization of hAT-MSCs

Primary cultured cells from adipose tissues were identified by characterization analysis of MSCs such as morphology, surface markers, and differentiation as previously described [14]. First, the morphology of the cells was observed through a microscope. Second, the cells were labelled with fluorescein isothiocyanate (FITC) or phycoerythrin (PE)-conjugated antibodies against CD14, CD34, CD73, CD90 (BD Biosciences Pharmingen, Heidelberg, Germany), CD45 or CD105 (Chemicon, Temecula, CA, USA) and then analyzed by a FACScan cytometer (BD Biosciences Pharmingen). Finally, the cells induced differentiation of adipocyte, chondrocyte, and osteocyte using a mesenchymal differentiation kit (Life Technologies) according to the manufacturer's instructions. The differentiated cells were verified by histologic staining using oil red O for adipogenic differentiation, alizarin red S for osteogenic differentiation and alcian blue for chondrogenic differentiation (Sigma- Aldrich). Only cells that fulfill the criteria of MSCs were used for further experiments.

2.3. Establishment of hAT-MSCs expressing sTRAIL

The synthesized sTRAIL DNA construct [14] was inserted into the pIRES2-EGFP vector [26] using restriction enzyme sites (Xho1/EcoR1) and confirmed by sequencing. pIRES2-EGFP.sTRAIL was transfected into hAT-MSCs by the Neon Transfection System (Life Technologies) [14,27]. The transfection efficiency was observed by real-time polymerase chain reaction (RT-PCR) for sTRAIL as described previously [14,28].

2.4. Determination of the median inhibitory concentration (IC_{50}) values of panobinostat

Cell viability was investigated using an EZ-Cytox cell viability assay kit (Daeil Lab Service Co, Seoul, Korea) according to the manufacturer's protocol. The cells ($2–4 \times 10^3$/well) were seeded in a 96-well microplate. After 24 h, panobinostat was administered at various concentrations for 48 h and 72 h, and the cells were then analyzed. In hAT-MSCs, cell viability analysis was performed by treating panobinostat for up to 96 h. DMSO-treated cells were used as controls. IC_{50} values were calculated using sigmoidal dose-response (variable slope) statistics and normalized in GraphPad Prism software. The IC_{50} value of panobinostat was used for further studies.

2.5. The cell surface expression of TRAIL receptors

FACS analysis of the cell surface expression of TRAIL receptors (DR4, DR5, DcR1, and DcR2) was performed by a FACSCalibur flow cytometer (Becton Dickinson Immunocytometry System, San Jose, CA). The cells (5×10^5) were treated with panobinostat for 48 h. The cells were incubated with 10 μg/mL anti-DR4, anti-DR5, anti-DcR1 and anti-DcR2 (BD Biosciences Pharmingen, San Diego, CA) per the manufacturer's recommendations. Mouse IgG1-PE and IgG2b-PE isotype controls (BD, negative control) were used to account for nonspecific interactions of antibodies with the cells. Negative controls omitting primary antibodies were run in parallel. The cells were washed twice and diluted in PBS at a concentration of 500 cells/μl for analysis. FACS analysis was repeated 3 times.

2.6. TRAIL enzyme-linked immunosorbent assay (ELISA)

To quantify the amount of TRAIL protein, hAT-MSCs or hAT-MSC.sTRAIL (3×10^5) were treated panobinostat for 48 h. The TRAIL protein was measured in the conditioned medium with a human TRAIL/TNFSF10 Quantikine ELISA kit (R&D systems, McKinley, MN, USA) according to the manufacturer's protocol.

2.7. Migration assay

hAT-MSCs or hAT-MSC.sTRAIL were treated panobinostat for 48 h. Tumor cells (5×10^4) were seeded to the lower chamber of a transwell support (8-μm pore size, Corning Costar, NY) and panobinostat-pretreated hAT-MSCs or hAT-MSC.sTRAIL (5×10^4) were added into the upper chamber in serum-free media and incubated 8 h. The transwell migration assay was performed as described previously [29]. The assays were performed in triplicate.

2.8. Co-culture of hAT-MSC.sTRAIL and malignant glioma cells

On day 0, tumor cells (1×10^3) were seeded in 96-well plates. On day 1, the cells were treated with panobinostat. On day 2, either hAT-MSCs or hAT-MSC.sTRAIL (3×10^3) were added to the culture. The cells were incubated for an additional 48 h, and the cell viability was investigated as described above.

2.9. Apoptosis analysis

Co-culture assays were performed in 8-well plate chambers. The number of apoptotic cells after combined treatment of hAT-MSC.sTRAIL with panobinostat was determined using a Click-iT terminal deoxynucleotidyl transferase dUTP nick end labeling (TUNEL) Alexa Fluor 594 kit following the manufacturer's instructions (Invitrogen). The cells were counterstained with DAPI to visualize the nuclei, and fluorescence images were obtained using a confocal microscope (Zeiss). The number of apoptotic cells was counted in three random fields.

2.10. Orthotopic xenograft malignant glioma mouse model: glioblastoma and diffuse midline glioma, H3 K27M-mutant model

All animal studies were approved by the Institutional Animal Care and Use Committee (IACUC) at Seoul National University (IACUC number: 15-0006-C1A0). Six-week-old female Bagg Albino/c nude (BALB/c-nu) mice were purchased from Central Lab Animal Inc. (Seoul, Korea). Mice were anesthetized by intraperitoneal (i.p.) injection of 20 mg/kg Zoletil and 10 mg/kg xylazine. Two independently designed orthotopic xenograft malignant glioma mouse models were introduced: glioblastoma using U87-enhanced firefly luciferase gene (U87-effLuc) and diffuse midline glioma, H3 K27M-mutant using DIPG XIII tumor cells. For the glioblastoma mouse model, U87 cells were prepared for imaging prior to injection. U87 tumor cells overexpressing the effLuc were generated using retroviral transfection and sorted by magnetic-activated cell sorting (MACS; Miltenyi Biotech Ltd., Bergisch-Gladbach, Germany). For the DIPG mouse model, DIPG XIII tumor cells were used. Each tumor cells (U87-effLuc or DIPG XIII, 4×10^4 in 3 μl PBS) were injected into the right pons as described previously [14]. The stereotactic coordinates were 1.5 mm to the right of the sagittal suture and on lambdoid suture at a 5.0 mm depth from the skull surface. Three days after tumor cell injection, the mice were randomized into six groups for treatment as follows (Supplementary Fig. S1): Group 1 = saline, Group 2 = panobinostat, Group 3 = hAT-MSCs, Group 4 = hAT-MSC.sTRAIL, Group 5 = hAT-MSCs + panobinostat, and Group 6 = hAT-MSC.sTRAIL + panobinostat. Saline or panobinostat (10 mg/kg) was administered by i.p. injection for 5 days, followed by a 2-day rest period [28,30]. Then, PBS, hAT-MSCs or hAT-MSC.sTRAIL (1.2×10^5 in 6 μl PBS) were stereotactically injected into the established tumor site. The treatment was repeated (Supplementary Fig. S1). The mice were perfused under deep anesthesia, and the brains were harvested for histological analysis. In the U87-effLuc tumor model, tumor volume (N = 7) was assessed 24 days after tumor cell injection, and the *in vivo* imaging and survival (N = 8) endpoint was 50 days. In the DIPG XIII tumor model, all mice (N = 12) were followed until the survival endpoint of 38 days. Tumor establishment in all euthanized mice was confirmed by necropsy.

2.11. Tumor volume and immunofluorescence analysis

Brain sections were stained with H&E for tumor volume analysis. Harvested brains were prepared in frozen tissue blocks as described in previous studies [14]. Brain sections were stained with primary antibodies including anti-Ac-H3 (1:100, Abcam), anti-Ki67 (1:200, Abcam), anti-cleaved caspase-3 antibody (1:50, Abcam), anti-Green fluorescent protein (GFP, 1:100, Santa Cruz Biotechnology, Paso Robles, CA), anti-DR4 (1:50, Abcam) or anti-DR5 (1:100, Abcam). GFP signals were amplified using anti-GFP. The secondary antibody, Alexa Fluor 488-conjugated goat anti-mouse IgG or anti-rabbit IgG (1:500, Invitrogen), was applied for 1 h. Slides were mounted with an antifading solution containing 4′-6′-diamidino-2-phenylindole (Vector Laboratories). Proliferation and apoptotic indices were analyzed as the percentage of positively stained cells in five randomly selected fields using a fluorescence microscope.

2.12. In vivo live imaging

Bioluminescence images (BLI) were acquired by the IVIS-100 imaging system (Xenogen Corporation, Alameda, CA). To acquire the BLI, the mice were injected with D-luciferin (150 mg/kg, Caliper Life Sciences, Hopkinton, MA, USA) intraperitoneally and anesthetized with 2% isoflurane in 100% O_2. The luminescence intensity in regions of interest (ROIs) from each image was quantified to examine the viability of the implanted cells [31].

2.13. Statistical analysis

All results are expressed as the means ± standard deviation (SD) or as the percentage of controls ± SD. Differences between two groups were analyzed by Student's t-test and differences between multiple groups were assessed using analysis of variance (ANOVA) with post-hoc Bonferroni test. The survival data are presented as Kaplan-Meier plots and were analyzed by the log-rank test. P-values < 0.05 were considered statistically significant. All experiments were conducted in triplicate.

3. Results

3.1. hAT-MSCs have characterization and differentiation of MSCs

Primary cultured cells from adipose-tissues were positive for the MSC markers, including CD73, CD90, and CD105, but negative for the hematopoietic markers CD14, CD34 and CD45 (Supplementary Fig. S2A). These cells displaying typical fibroblast-like morphology were differentiated into the adipocyte, osteocyte, and chondrocyte, respectively (Supplementary Fig. S2B). These results suggest that the primary cultured cells were hAT-MSCs.

3.2. Panobinostat inhibits malignant glioma cell growth

After panobinostat treatment at various doses, we conducted cell viability tests on primary cultured glioblastoma cells (SNUH.GBM1 and SNUH.GBM2), diffuse midline glioma, H3 K27M-mutant cells (DIPG XIII and DIPG XIX) and glioblastoma cell lines (U87 and U251). In all tested malignant glioma cells, cell viability was significantly decreased on day 3. We calculated the IC_{50} values of panobinostat at 72 h: 0.11 ± 0.09 μM for SNUH.GBM1, 1.4 ± 0.82 μM for SNUH.GBM2, 0.23 ± 0.14 μM for DIPG XIII, 0.06 ± 0.02 μM for DIPG XIX, 0.03 ± 0.001 μM for U87 and 0.04 ± 0.02 μM for U251 (Fig. 1). The decreased viability was more dramatic in diffuse midline glioma, H3 K27M-mutant cells than in primary glioblastoma cells. Panobinostat showed no discernible effect on the viability of hAT-MSCs and hAT-MSC.sTRAIL; IC_{50} values under 50 μM were not achieved in both cells up to 96 h (Supplementary Fig. S3A).

3.3. Panobinostat induces the expression of TRAIL DRs in brain tumor cells but not in hAT-MSCs and hAT-MSC.sTRAIL

The effects of panobinostat on the expression level of TRAIL DRs and DcRs were tested in malignant glioma cells at each IC_{50} value. All malignant glioma cells showed significantly increased expression of DR4 up to 17.8-fold (17.8 ± 4.7-fold in SNUH.GBM2, 2.0 ± 0.3-fold in U87 and 17.1 ± 2.3-fold in U251) or of DR5 up to 5.9-fold (5.9 ± 1.7-fold in SNUH.GBM1, 4.0 ± 1.6-fold in SNUH.GBM2, 2.2 ± 0.4-fold in DIPG XIII, 2.7 ± 0.8-fold in DIPG XIX and 4.4 ± 1.3-fold in U251), indicating the potential of panobinostat in future therapeutic approaches (Fig. 2 and Supplementary Table S1). On the other hand, the effects of panobinostat on the expression of DcRs were not evident. Importantly, the expression of DRs in hAT-MSCs and hAT-MSC.sTRAIL was not affected by 1.4 μM of panobinostat treatment (DR4: 1.1 ± 0.2-fold in hAT-MSCs and 0.98 ± 0.7-fold in hAT-

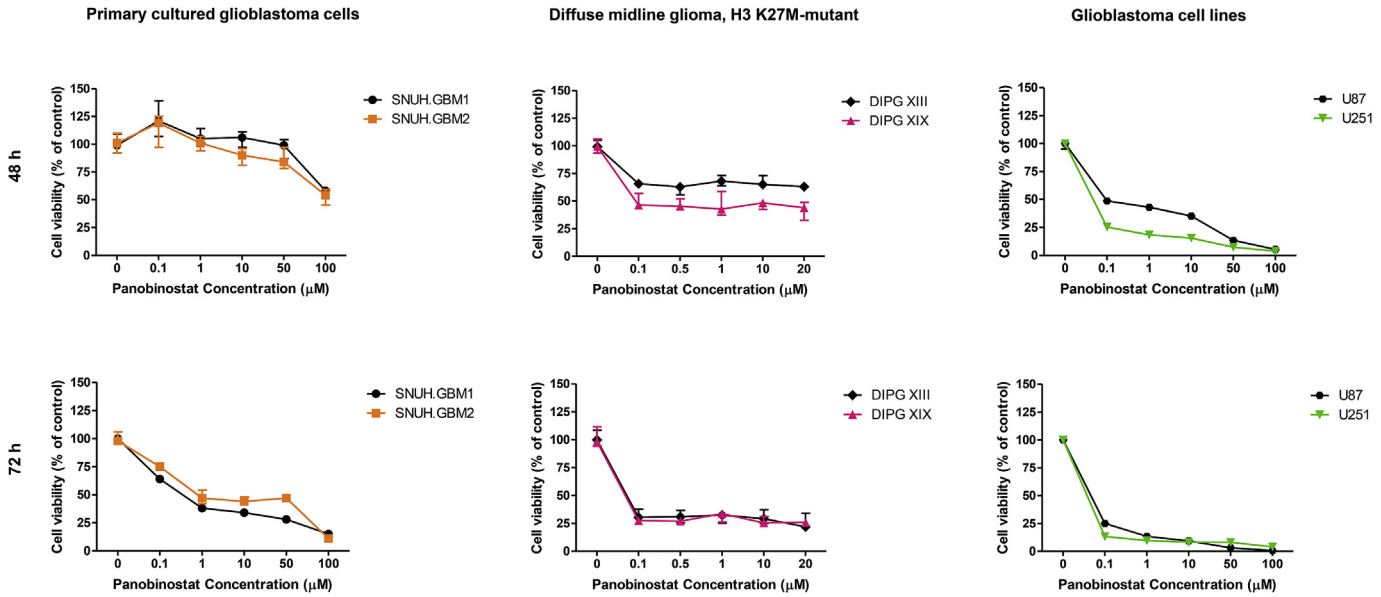

Fig. 1. Growth analysis of malignant glioma cells after treatment with panobinostat. Cell viability was determined 48 and 72 h after panobinostat treatment at various doses. The analysis graphs show significant suppression of cell viability in primary cultured glioblastoma cells (SNUH.GBM1 and SNUH.GBM2), diffuse midline glioma, H3 K27M-mutant cells (DIPG XIII and DIPG XIX) and glioblastoma cell lines (U87 and U251). The efficacy of panobinostat is illustrated in dose and time –dependent manner (IC50 range, 0.03–0.14 μM). IC50 values were calculated using sigmoidal dose-response (variable slope) statistics and normalized in GraphPad Prism software.

MSC.sTRAIL; DR5: 0.97 ± 0.3-fold in hAT-MSCs and 0.97 ± 0.4-fold in hAT-MSC.sTRAIL; Supplementary Fig. S3B, Supplementary Table S1).

3.4. Panobinostat does not suppress sTRAIL expression and migration of hAT-MSC.sTRAIL in vitro and in vivo

We also confirmed the impact of panobinostat on tumor-homing ability and sTRAIL secretion level of hAT-MSC and hAT-MSC.sTRAIL. We found that hAT-MSCs and hAT-.MSC.sTRAIL showed no significant difference in the secretion level (Supplementary Fig. S4) and migration ability after panobinostat treatment *in vitro* (Supplementary Fig. S5). In addition, *in vivo* U87-effLuc tumor model, hAT-MSC.sTRAIL was also observed not only at the site of initial injection but also at the border between tumor and normal parenchyma. Even when treated with panobinostat, there was no significant change in the distribution pattern

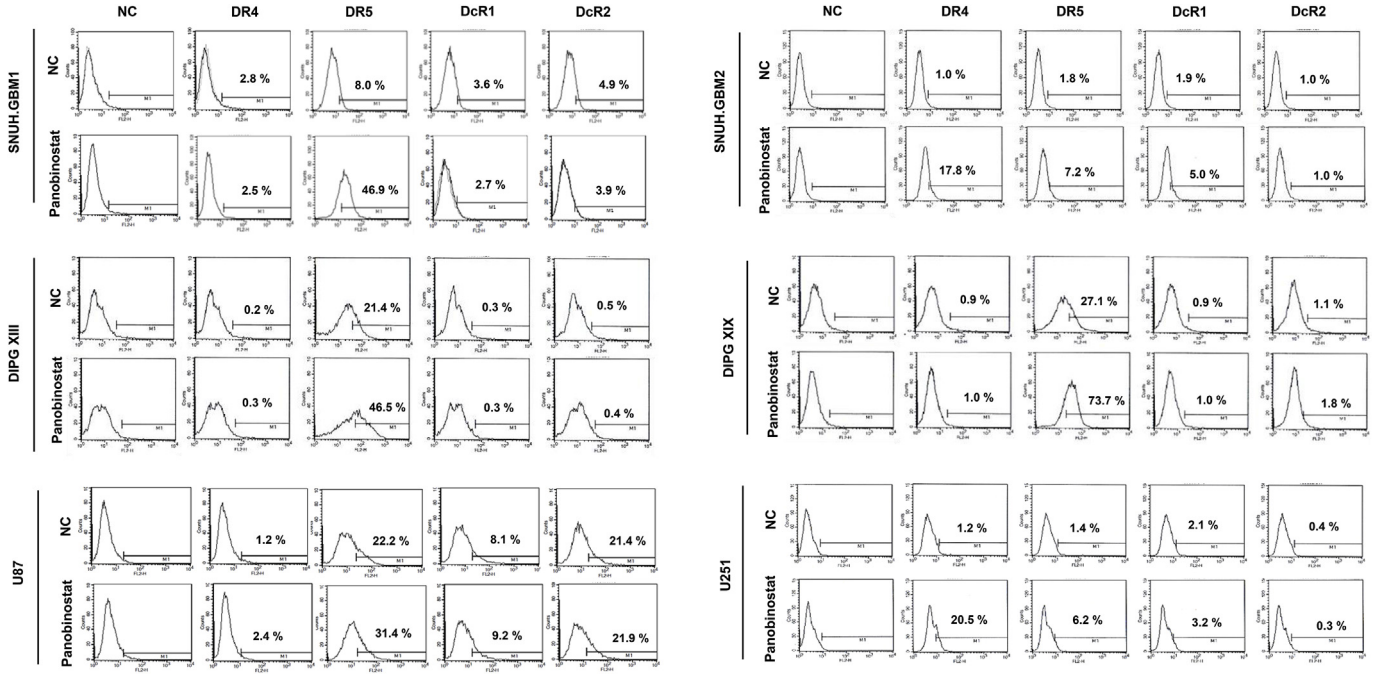

Fig. 2. The expression of tumor necrosis factor-related apoptosis-inducing ligand (TRAIL) receptors after panobinostat treatment in malignant glioma cells (glioblastoma, diffuse midline glioma, H3 K27M-mutant cells and glioblastoma cell lines). Surface death receptors (DR) 4, DR5, decoy receptors (DcR) 1, and DcR2 level in panobinostat treated malignant glioma cells was determined by flow cytometry with using a PE-conjugated antibody and a control IgG (negative control). Histograms obtained in a representative experiment are shown. (B) The graph represents quantified fluorescence intensity for cell surface DR4, DR5, DcR1, and DcR2 expression. Panobinostat induced the expression of DR 4 and DR5 in all malignant glioma cells. There were no effects of panobinostat on the expression of DcR 1 and DcR2.

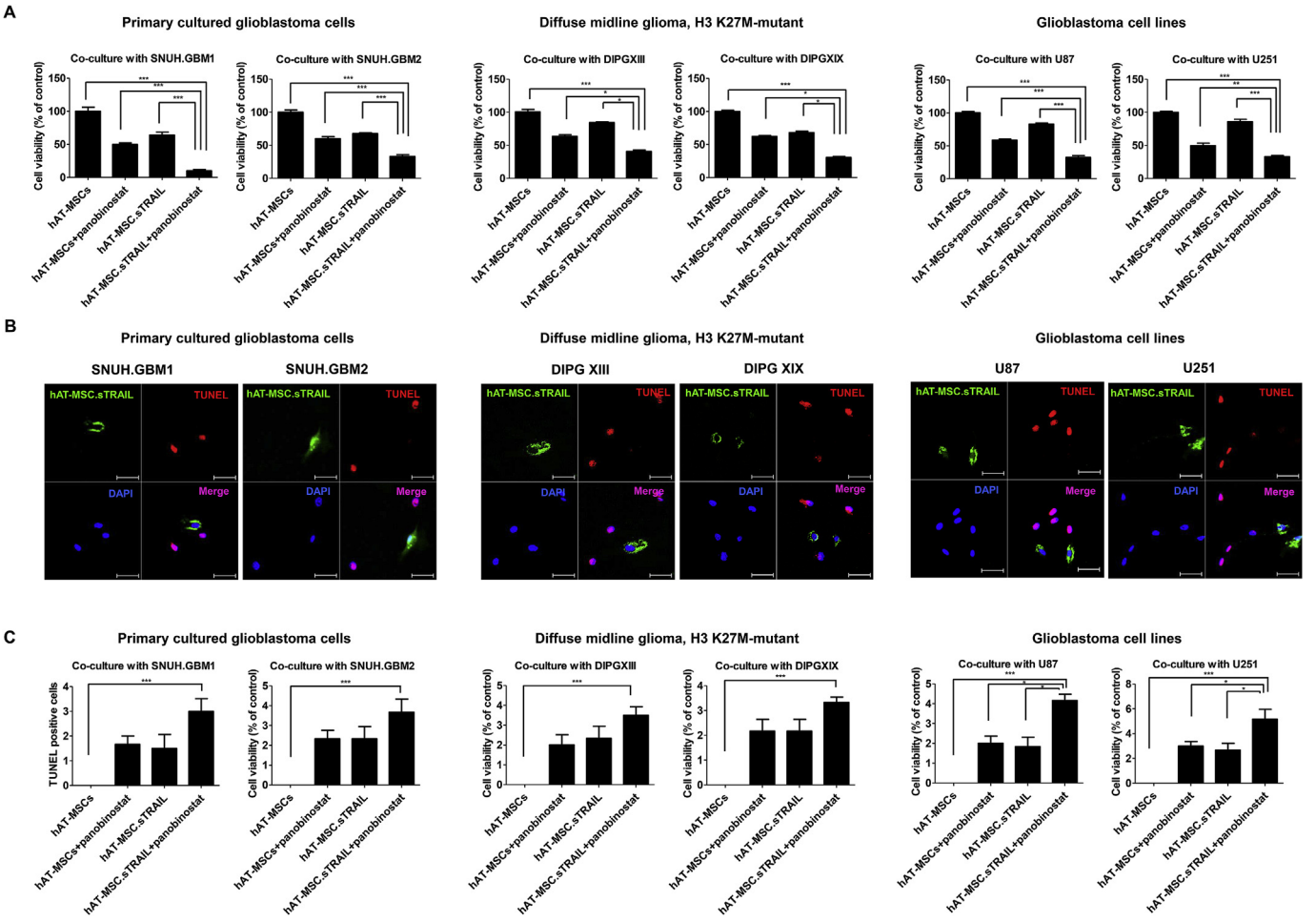

Fig. 3. The anti-cancer effects of combined treatment with hAT-MSC.sTRAIL and panobinostat in malignant glioma cells *in vitro*. Each glioblastoma, diffuse midline glioma, H3 K27M-mutant cells, and glioblastoma cell lines were co-cultured with hAT-MSCs, hAT-MSCs + panobinostat, hAT-MSC.sTRAIL, hAT-MSC.sTRAIL + panobinostat, respectively. IC50 of panobinostat was applied in corresponding groups. (A) Panobinostat was applied to each malignant glioma cell and co-cultured with hAT-MSCs or hAT-MSC.sTRAIL. Combined treatment of hAT-MSC.sTRAIL with panobinostat significantly decreased the cell viability compared to that of control and single treatment groups. *P < 0.05, **P < 0.01, ***P < 0.001. (B) TUNEL assays showed apoptotic cell death in malignant glioma cells but not in hAT-MSCs and hAT-MSC.sTRAIL. The apoptotic cell proportion was increased in all malignant glioma cells after combined treatment with hAT-MSC.sTRAIL and panobinostat. Cells were counterstained with DAPI (blue). hAT-MSC.sTRAIL-GFP (green), TUNEL (red), Scale bars = 50 μm. Differences among were hAT-MSCs, hAT-MSCs + panobinostat, hAT-MSC.sTRAIL, hAT-MSC.sTRAIL + panobinostat analyzed using One-Way ANOVA with post-hoc Tukey's tests. Asterisks represented the significance levels: *P < 0.05, **P < 0.01, ***P < 0.001. (For interpretation of the references to colour in this figure legend, the reader is referred to the Web version of this article.)

of the hAT-MSC.sTRAIL *in vivo* (Supplementary Fig. S6).

3.5. Combined treatment of hAT-MSC.sTRAIL with panobinostat enhances apoptosis

Next, we evaluated the therapeutic efficacy of the combined treatment of hAT-MSC.sTRAIL with panobinostat. The cell viability was significantly suppressed in all malignant glioma cells with combined treatment of hAT-MSC.sTRAIL with panobinostat compared to other treatment groups (Fig. 3A). After panobinostat treatment of the co-culture system, apoptosis was induced in malignant glioma cells but not in hAT-MSCs or hAT-MSC.sTRAIL (Fig. 3B). The number of apoptotic cells was increased in the hAT-MSC.sTRAIL with panobinostat group compared with the hAT-MSC only group (Fig. 3C). Taken together, these results indicate enhancement of apoptotic cell death in all malignant glioma cells after the combined treatment of hAT-MSC.sTRAIL with panobinostat.

3.6. Combined treatment of hAT-MSC.sTRAIL with panobinostat reduces tumor volume in U87-effLuc model

We adopted a previously designed glioblastoma mouse model using U87-effLuc cells [15] to demonstrate the *in vivo* therapeutic efficacy of combined treatment of hAT-MSC.sTRAIL with panobinostat. Experimental groups and time schedules are shown in Supplementary Fig. S1. Histological analysis revealed that tumor volume was significantly decreased with combined treatment of hAT-MSC.sTRAIL with panobinostat (Group 6, 19.1 ± 4.0 mm^3) compared to other groups (Group 1, 47.7 ± 6.0 mm^3, P < 0.001; Group 2, 40.3 ± 8.0 mm^3, P < 0.001; Group 3, 39.2 ± 8.7 mm^3, P < 0.001; Group 4, 32.0 ± 7.1 mm^3, P < 0.01; and Group 5, 33.1 ± 6.1 mm^3, P < 0.01; Fig. 4) in the U87-effLuc tumor model. We next investigated the number of Ac-H3-positive cells, the proliferation rate of cells and the induction of apoptosis in cells by immunofluorescence analysis. Combined treatment of hAT-MSC.sTRAIL with panobinostat increased the number of Ac-H3-positive cells, decreased the number of Ki-67-positive cells and increased the number of cleaved caspase-3-positive cells (Fig. 4). In addition, we observed an increase level of DR4 and DR5 in panobinostat

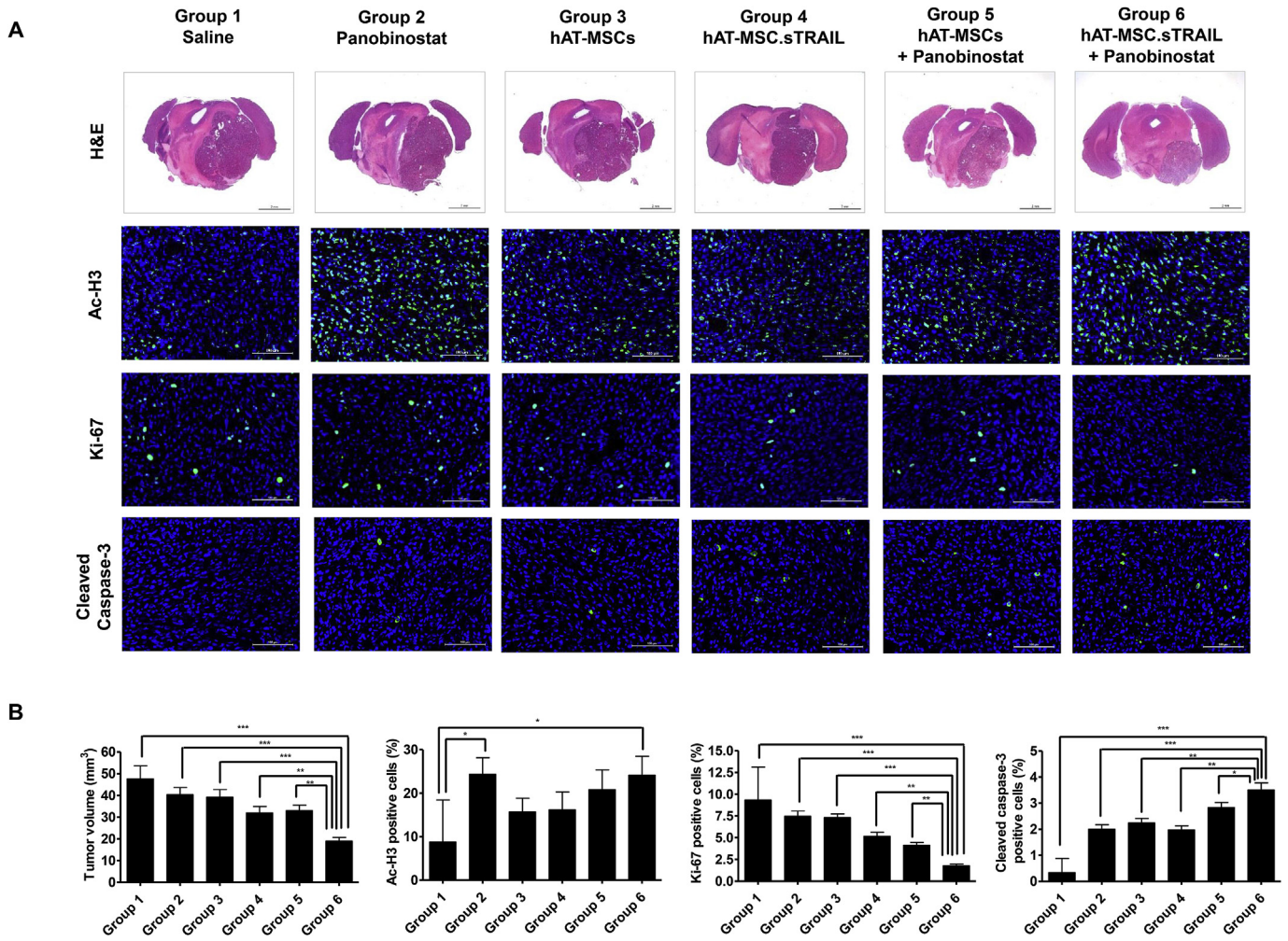

Fig. 4. Short-term therapeutic efficacy of combined treatment with hAT-MSC.sTRAIL and panobinostat in U87-effLuc tumor models. Representative histological images show a reduction in tumor volume by combined treatment with hAT-MSC.sTRAIL and panobinostat compared with other treatment groups. Hematoxylin and eosin (H&E) staining is shown. Scale bars = 2 mm. Representative immunofluorescence images show Ac-H3, Ki-67, and cleaved caspase-3 protein levels. The images show that the combined treatment of hAT-MSC.sTRAIL with panobinostat increased the number of Ac-H3-positive cells, decreased the number of Ki-67-positive cells and increased the number of cleaved caspase-3-positive cells. Positive cells are shown in green. Cells were counterstained with DAPI (blue). Scale bars = 100 μm. Differences between multiple groups were assessed by using a Two-Way ANOVA with post-hoc Bonferroni tests. Asterisks represent statistically significant changes; *P < 0.05, **P < 0.01, ***P < 0.001. (For interpretation of the references to colour in this figure legend, the reader is referred to the Web version of this article.)

treated group (Supplementary Fig. S7). These results showed that combined treatment of hAT-MSC.sTRAIL with panobinostat is more effective than the control or single treated groups.

3.7. Combined treatment of hAT-MSC.sTRAIL with panobinostat prolongs survival in U87-effLuc and DIPG III model

BLI was performed to visualize the therapeutic effects of combined treatments *in vivo*. Images were obtained serially before, during, and after two cycles of hAT-MSC.sTRAIL with panobinostat. From the serial measurements of tumor-occupied areas, the combined treatment of hAT-MSC.sTRAIL with panobinostat showed the most prominent decreases in tumor size compared to other treatment groups. U87-effLuc tumor cell growth was markedly diminished after combined treatment with hAT-MSC.sTRAIL and panobinostat (Group 6, $8.1 \pm 0.4 \times 10^6$ p/sec/cm^2/sr) compared to other treatment groups at day 18 (Group 1, $23.6 \pm 1.5 \times 10^6$ p/sec/cm^2/sr, $P < 0.001$; Group 2, $18.9 \pm 2.4 \times 10^6$ p/sec/cm^2/sr, $P < 0.001$; Group 3, $18.8 \pm 2.1 \times 10^6$ p/sec/cm^2/sr, $P < 0.001$; Group 4, $14.4 \pm 2.1 \times 10^6$ p/sec/cm^2/sr, $P < 0.001$; Group 5, $19.0 \pm 2.3 \times 10^6$ p/sec/cm^2/sr, $P < 0.001$; Fig. 5A and B and Supplementary Table S2).

The long-term therapeutic efficacy of treatment on U87-effLuc and DIPG XIII cells was determined by monitoring the survival of animals from all treatment groups. In glioblastoma mouse model using U87-effLuc cells, survival analyses displayed significant survival benefits for U87-effLuc tumor model and that received the combined treatment of hAT-MSC.sTRAIL with panobinostat (Group 6, 34 d) compared to other groups (Group 1, 21 d, $p = 0.004$; Group 2, 20 d, $p = 0.002$; Group 3, 22 d, $p = 0.011$; Group 4, 25 d, $p = 0.023$; and Group 5, 22 d, $p = 0.019$; Fig. 5C). In diffuse midline glioma, H3 K27M-mutant mouse model using DIPG XIII cells, combined treatment of hAT-MSC.sTRAIL with panobinostat showed survival advantages for DIPG XIII tumor model (Group 6, 29.5 d) compared to other groups (Group 1, 21 d, $p < 0.0001$; Group 2, 21 d, $p = 0.0005$; Group 3, 21.5 d, $p = 0.001$; Group 4, 24 d, $p = 0.479$; and Group 5, 22 d, $p = 0.011$; Fig. 5D). Although survival between Group 4 and Group 6 was not statistically significant, Group 6 showed extended median survival by 5.5 days compared to Group 4. No major systemic toxicities were observed.

4. Discussion

In this study, we demonstrate that panobinostat has strong anti-cancer effects and induces DR expression in malignant gliomas

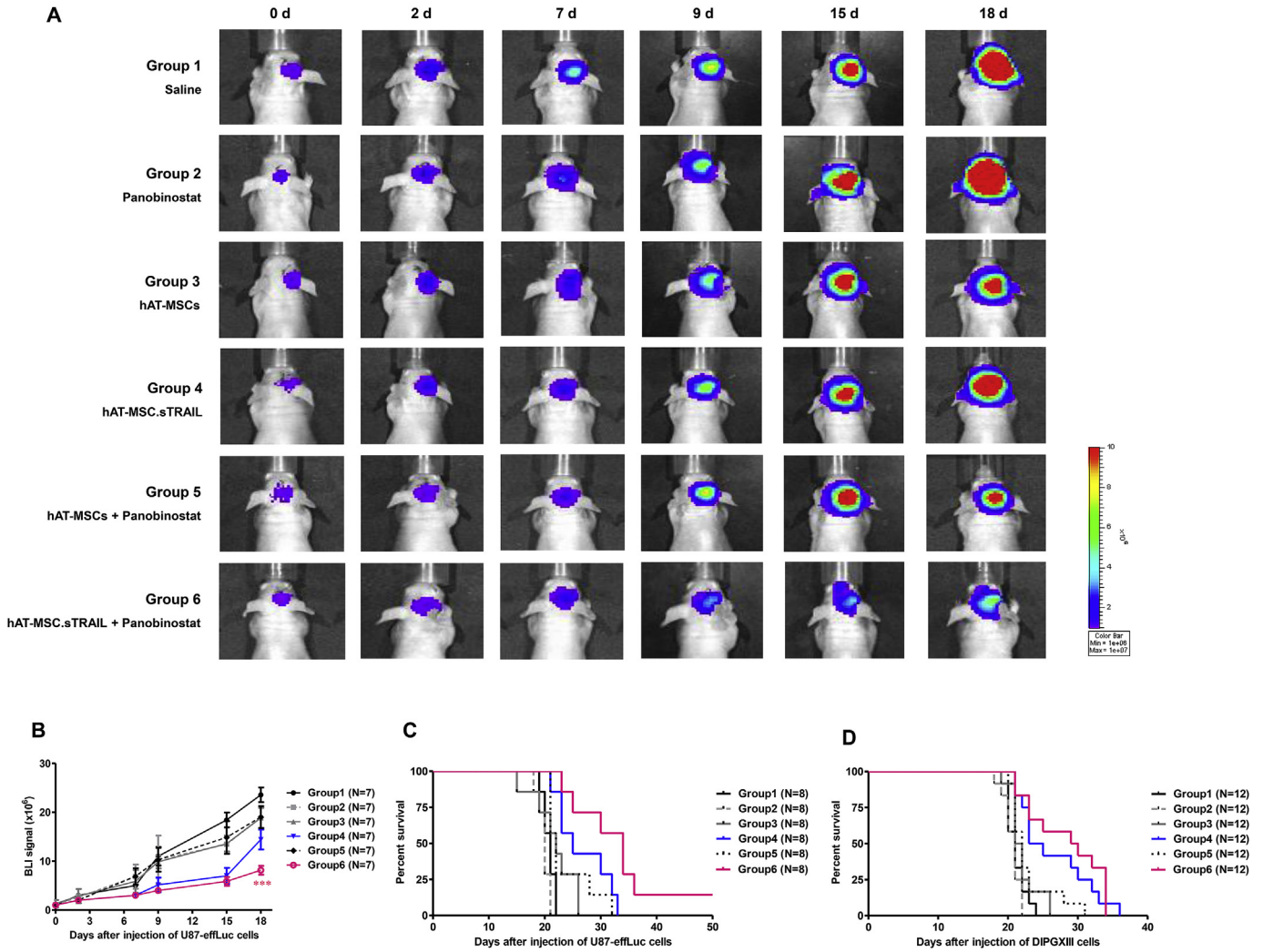

Fig. 5. Long-term therapeutic efficacy of combined treatment with hAT-MSC.sTRAIL and panobinostat in U87-effLuc and DIPGXIII tumor models. (A) Representative *in vivo* live imaging of implanted U87-effLuc tumor cells after treatment by the IVIS-100 imaging system. (B) Quantification of serial bioluminescence imaging (BLI) of tumor-occupied areas from *in vivo* live imaging. ***P $<$ 0.001. Kaplan-Meier plots and log- rank tests in orthotopic xenograft diffuse intrinsic pontine glioma (DIPG) mouse model using (C) U87-effLuc cells (N = 8) and (D) DIPG XIII cells (N = 9). In U87-effLuc tumor model, the combined treatment groups (Group 6, 34 d) prolong the survival rate compared to other groups (Group 1, 21 d, p = 0.004; Group 2, 20 d, p = 0.002; Group 3, 22 d, p = 0.011; Group 4, 25 d, p = 0.023; and Group 5, 22 d, p = 0.019). In DIPG XIII tumor model, the median survival of Group 6 was 5.5 days longer compared to Group 4 although survival between Group 4 and Group 6 was not statistically significant (Group 1, 21 d, p $<$ 0.0001; Group 2, 21 d, p = 0.0005; Group 3, 21.5 d, p = 0.001; Group 4, 24 d, p = 0.479; and Group 5, 22 d, p = 0.011).

including glioblastoma and diffuse midline glioma, H3 K27M-mutant. We employed two models in this experiment: U87 for glioblastoma and DIPG XIII for diffuse midline glioma, H3 K27M-mutant. Interestingly, panobinostat does not affect DR expression in hAT-MSCs. We also confirm that combined treatment of panobinostat with hAT-MSC.sTRAIL significantly reduces the tumor volume in the U87-effLuc mouse model and prolongs the survival in both U87-effLuc and DIPG XIII mouse model.

Previously, we investigated the therapeutic potential of stem cell-based gene therapy using hAT-MSC.sTRAIL [25,26,32,33]. We confirmed their extensive migratory potential and therapeutic efficacy against various malignant glioma cells *in vitro* and *in vivo*. However, the therapeutic effects of TRAIL may have been impeded by TRAIL resistance and low expression of DRs in malignant glioma cells. Our previous study on MSC.sTRAIL therapy was likewise challenged by decreased TRAIL sensitivity shortly after treatment [14]. Thereafter, many studies have evaluated TRAIL-sensitizing strategies through the combination of TRAIL with gemcitabine [33], platinums [33,34], doxorubicin [35], irinotecan [36], 5-FU [36] or radiation therapy [37,38]. The strategy behind combined therapies is to enhance the therapeutic effects by simultaneously targeting multiple mechanisms, thus requiring a lower dose to prevent adverse side effects. Despite these efforts, combined therapy faces complications such as systemic toxicities, short biological half-lives of the drugs, and unstandardized delivery methods, which make it difficult for clinical application [38,39].

In the present study, we adopted a strategy of modifying the phenotype of malignant glioma cells via epigenetic modulation. We used pan-HDACi to induce the expression of TRAIL DRs in malignant glioma cells. HDACi is known to sensitize TRAIL by inducing DR4 and DR5 expression through activation of NF-kB and of pro-apoptotic members of the Bcl-2 family [16–18]. In the present study, panobinostat significantly induced the expression of DRs in malignant glioma cells (up to 17.8-fold with DR4 and up to 5.9-fold with DR5). This increased expression of DRs led to the enhanced apoptosis of malignant glioma cells. Furthermore, panobinostat did not affect the viability and DR expression of hAT-MSCs and hAT-MSC.sTRAIL within the therapeutic dosage range against malignant glioma cells.

Among HDACi, panobinostat has been reported to be the most effective agent against DIPG by functional drug screening and pre-clinical studies [7]. Targeted therapy with panobinostat has recently entered phase I clinical trials for the treatment of children with recurrent or progressive DIPG [7,40]. However, the therapeutic dose of panobinostat needs to be titrated due to the systemic toxicity associated with the administration of pan-HDACi [40]. A preclinical study using both genetic and orthotopic xenograft DIPG models showed that extended consecutive daily treatment with 10 or 20 mg/kg panobinostat consistently led to significant toxicity. However, reduced well-tolerated doses of panobinostat did not show a survival benefit compared to vehicle-treated mice [41].

We pursued a higher therapeutic efficacy using a combination of hAT-MSC.sTRAIL and panobinostat treatments based on two known outcomes of panobinostat treatment: induction of TRAIL DR expression and targeting of the epigenetic dysregulation in malignant glioma cells. However, our treatment did not achieve a complete cure. Therefore, other histone modifications or alternative therapeutic delivery methods should be explored for further clinical development of this therapy for patients with malignant gliomas.

The combined therapy in U87-effLuc model significantly prolonged survival. However, it was not as effective in DIPG XIII model. This result might be due to the marked difference of DIPG from adult high- grade glioma at a phenotypic and molecular level [6]. The other explanation is that DIPG XIII cells were obtained from autopsy tissue, therefore is not treatment-naïve. The drug response may be different from the cells collected from the fresh tissues at the time of presentation. Recently, off-target proteins such as AMDHD2, CUTA, GLO1, GNPADA1, LOC153365, PAH, and TTC38 by panobinostat have been proposed therefore this should be considered when using panobinostat as therapeutic agents [41].

5. Conclusion

Combined treatment of hAT-MSC.sTRAIL with panobinostat potentiates anti-cancer effects both *in vitro* and *in vivo* and deserves consideration for future clinical applications against malignant gliomas.

Funding

This study was supported by grant number 3420140080 from the SK Telecom Research Fund.

Conflicts of interest

The authors declare that there are no conflicts of interest in regard to this study.

Appendix A. Supplementary data

Supplementary data to this article can be found online at https://doi.org/10.1016/j.canlet.2018.10.012.

References

[1] P.Y. Wen, S. Kesari, Malignant gliomas in adults, N. Engl. J. Med. 359 (2008) 492–507.
[2] C.P. Haar, P. Hebbar, GCt Wallace, et al., Drug resistance in glioblastoma: a mini review, Neurochem. Res. 37 (2012) 1192–1200.
[3] S. Khatua, K.R. Moore, T.S. Vats, J.R. Kestle, Diffuse intrinsic pontine glioma-current status and future strategies, Childs Nerv. Syst. 27 (2011) 1391–1397.
[4] D. Hargrave, U. Bartels, E. Bouffet, Diffuse brainstem glioma in children: critical review of clinical trials, Lancet Oncol. 7 (2006) 241–248.
[5] R.K. Mathew, J.T. Rutka, Diffuse intrinsic pontine glioma: clinical features, molecular genetics, and novel targeted therapeutics, J. Kor. Neurosurg. Soc. 61 (2018) 343–351.
[6] D.N. Louis, A. Perry, G. Reifenberger, et al., The 2016 World Health organization classification of tumors of the central nervous system: a summary, Acta Neuropathol. 131 (2016) 803–820.
[7] C.S. Grasso, Y. Tang, N. Truffaux, et al., Functionally defined therapeutic targets in diffuse intrinsic pontine glioma, Nat. Med. 21 (2015) 827.
[8] P.W. Lewis, M.M. Muller, M.S. Koletsky, et al., Inhibition of PRC2 activity by a gain-of-function H3 mutation found in pediatric glioblastoma, Science (New York, NY) 340 (2013) 857–861.
[9] R. Hashizume, N. Andor, Y. Ihara, et al., Pharmacologic inhibition of histone demethylation as a therapy for pediatric brainstem glioma, Nat. Med. 20 (2014) 1394–1396.
[10] C. Kasuga, T. Ebata, N. Kayagaki, et al., Sensitization of human glioblastomas to tumor necrosis factor-related apoptosis-inducing ligand (TRAIL) by NF-kappaB inhibitors, Cancer Sci. 95 (2004) 840–844.
[11] A.D. Sanlioglu, E. Dirice, C. Aydin, N. Erin, S. Koksoy, S. Sanlioglu, Surface TRAIL decoy receptor-4 expression is correlated with TRAIL resistance in MCF7 breast cancer cells, BMC Canc. 5 (2005) 54.
[12] A. Panner, A.T. Parsa, R.O. Pieper, Translational regulation of TRAIL sensitivity, Cell Cycle 5 (2006) 147–150.
[13] R.W. Johnstone, A.J. Frew, M.J. Smyth, The TRAIL apoptotic pathway in cancer onset, progression and therapy, Nat. Rev. Canc. 8 (2008) 782–798.
[14] S.A. Choi, Y.E. Lee, P.A. Kwak, et al., Clinically applicable human adipose tissue-derived mesenchymal stem cells delivering therapeutic genes to brainstem gliomas, Cancer Gene Ther. 22 (2015) 302–311.
[15] A.J. Frew, R.K. Lindemann, B.P. Martin, et al., Combination therapy of established cancer using a histone deacetylase inhibitor and a TRAIL receptor agonist, Proc. Natl. Acad. Sci. U.S.A. 105 (2008) 11317–11322.
[16] S. Schuler, P. Fritsche, S. Diersch, et al., HDAC2 attenuates TRAIL-induced apoptosis of pancreatic cancer cells, Mol. Canc. 9 (2010) 80.
[17] T.R. Singh, S. Shankar, R.K. Srivastava, HDAC inhibitors enhance the apoptosis-inducing potential of TRAIL in breast carcinoma, Oncogene 24 (2005) 4609–4623.
[18] M. Cornago, C. Garcia-Alberich, N. Blasco-Angulo, et al., Histone deacetylase inhibitors promote glioma cell death by G2 checkpoint abrogation leading to mitotic catastrophe, Cell Death Dis. 5 (2014) e1435.
[19] A.R. Jazirehi, S.K. Kurdistani, J.S. Economou, Histone deacetylase inhibitor sensitizes apoptosis-resistant melanomas to cytotoxic human T lymphocytes through regulation of TRAIL/DR5 pathway, J. Immunol. 192 (2014) 3981–3989.
[20] E. Adamopoulou, U. Naumann, HDAC inhibitors and their potential applications to glioblastoma therapy, OncoImmunology 2 (2013) e25219.
[21] J.K. Earel Jr., R.L. VanOosten, T.S. Griffith, Histone deacetylase inhibitors modulate the sensitivity of tumor necrosis factor-related apoptosis-inducing ligand-resistant bladder tumor cells, Cancer Res. 66 (2006) 499–507.
[22] K.P. Garnock-Jones, Panobinostat: first global approval, Drugs 75 (2015) 695–704.
[23] N.H. Pipalia, C.C. Cosner, A. Huang, A. Chatterjee, P. Bourbon, N. Farley, P. Helquist, O. Wiest, F.R. Maxfield, Histone deacetylase inhibitor treatment dramatically reduces cholesterol accumulation in Niemann-Pick type C1 mutant human fibroblasts, Proc. Natl. Acad. Sci. U. S. A. 108 (2011) 5620–5625.
[24] S.A. Choi, J.Y. Lee, J.H. Phi, et al., Identification of brain tumour initiating cells using the stem cell marker aldehyde dehydrogenase, Eur. J. Canc. 50 (2014) 137–149.
[25] S. Catherine, T. Yujie, T. Nathalene, et al., Functionally defined therapeutic targets in diffuse intrinsic pontine glioma, Nat. Med. 21 (6) (2015) 555–559.
[26] S.A. Choi, S.K. Hwang, K.C. Wang, et al., Therapeutic efficacy and safety of TRAIL-producing human adipose tissue-derived mesenchymal stem cells against experimental brainstem glioma, Neuro Oncol. 13 (2011) 61–69.
[27] S.A. Choi, J.W. Yun, K.M. Joo, et al., Preclinical biosafety evaluation of genetically modified human adipose tissue-derived mesenchymal stem cells for clinical applications to brainstem glioma, Stem Cell. Dev. 25 (2016) 897–908.
[28] M.C. Crisanti, A.F. Wallace, V. Kapoor, et al., The HDAC inhibitor panobinostat (LBH589) inhibits mesothelioma and lung cancer cells in vitro and in vivo with particular efficacy for small cell lung cancer, Mol. Canc. Therapeut. 8 (2009) 2221–2231.
[29] S.A. Choi, J.Y. Lee, S.E. Kwon, et al., Human adipose tissue-derived mesenchymal stem cells target brain tumor-initiating cells, PLoS One 28 (2015) e013287710(7).
[30] J.H. Phi, S.A. Choi, P.A. Kwak, et al., Panobinostat, a histone deacetylase inhibitor, suppresses leptomeningeal seeding in a medulloblastoma animal model, Oncotarget 24 (2017) 56747–56757.
[31] S.A. Choi, P.A. Kwak, S.K. Kim, et al., In vivo bioluminescence imaging for leptomeningeal dissemination of medulloblastoma in mouse models, BMC Canc. 16 (2016) 723.
[32] L.G. Menon, K. Kelly, H.W. Yang, S.K. Kim, P.M. Black, R.S. Carroll, Human bone marrow-derived mesenchymal stromal cells expressing S-TRAIL as a cellular delivery vehicle for human glioma therapy, Stem Cell. 27 (2009) 2320–2330.
[33] C.H. Mom, J. Verweij, C.N. Oldenhuis, et al., Mapatumumab, a fully human agonistic monoclonal antibody that targets TRAIL-R1, in combination with gemcitabine and cisplatin: a phase I study, Clin. Canc. Res. Official J. Am. Assoc. Canc. Res. 15 (2009) 5584–5590.
[34] S. Shamimi-Noori, W.S. Yeow, M.F. Ziauddin, et al., Cisplatin enhances the anti-tumor effect of tumor necrosis factor-related apoptosis-inducing ligand gene therapy via recruitment of the mitochondria-dependent death signaling pathway, Cancer Gene Ther. 15 (2008) 356–370.
[35] A. El-Zawahry, J. McKillop, C. Voelkel-Johnson, Doxorubicin increases the effectiveness of Apo2L/TRAIL for tumor growth inhibition of prostate cancer xenografts, BMC Canc. 5 (2005) 2.
[36] B. Sikic, H. Wakelee, M. Von Mehren, et al., A Phase 1b study to assess the safety of lexatumumab, a human monoclonal antibody that activates TRAIL-R2, in combination with gemcitabine, pemetrexed, doxorubicin or FOLFIRI, Mol. Canc. Therapeut. 6 (2007) B72-B72.
[37] J. Lemke, S. von Karstedt, J. Zinngrebe, H. Walczak, Getting TRAIL back on track

for cancer therapy, Cell Death Differ. 21 (2014) 1350–1364.
[38] S.M. Kim, J.H. Oh, S.A. Park, et al., Irradiation enhances the tumor tropism and therapeutic potential of tumor necrosis factor-related apoptosis-inducing ligand-secreting human umbilical cord blood-derived mesenchymal stem cells in glioma therapy, Stem Cell. 28 (2010) 2217–2228.
[39] A. Ashkenazi, P. Holland, S.G. Eckhardt, Ligand-based targeting of apoptosis in cancer: the potential of recombinant human apoptosis ligand 2/Tumor necrosis factor-related apoptosis-inducing ligand (rhApo2L/TRAIL), J. Clin. Oncol. Official J. Am. Soc. Clin. Oncol. 26 (2008) 3621–3630.
[40] T. Hennika, G. Hu, N.G. Olaciregui, et al., Pre-clinical study of panobinostat in xenograft and genetically engineered murine diffuse intrinsic pontine glioma models, PLoS One 12 (2017) e0169485.
[41] I. Becher, T. Werner, C. Doce, et al., Thermal profiling reveals phenylalanine hydroxylase as an off-target of panobinostat, Nat. Chem. Biol. 12 (2016) 908–910.